

Simulation and Comparison Research of Lagrange and Kane Dynamics Modeling for The 4-DOF Modular Industrial Robot

Xiao Li^{1,a}, Hanxu Sun^{2,b}, Linjing Liao^{2,c}, Jingzhou Song^{2,d}

¹School of Mechanical Engineering and Automation, Beihang University, in China

²School of Automation, Beijing University of Posts and Telecommunication, in China

^alxwshy@163.com, ^bhxsun@bupt.edu.cn, ^c604337834@qq.com, ^dsjz2008@bupt.edu.cn

Key words: Modular industrial robot, Dynamics modeling, Dynamics simulation.

Abstract. Based on joint parameter and robot configuration, the Lagrange and Kane dynamics modeling are established for the 4-DOF modular industrial robot in this paper. The planning mission was performed in the Lagrange dynamics modeling and Kane dynamics modeling by simulation software. The simulation results shown that the Kane model is better than the Lagrange model in the 4-DOF robot. And the Kane model has better execution effect when the joint torque is greater.

Introduction

With the rising number of industrial robot installed, modular industrial robots have achieved high-speed development. Dynamic model has great effect on the dynamic characteristics of robot. Dynamic modeling method have many methods, such as Newton-Euler method[1], Lagrange method[2], Kane method[3-4], the principle of virtual work method[5], screw and dual-number method [6], etc. Based on the 4-Dof modular robot, respectively, establish the Lagrange dynamic model and Kane dynamic model under the condition of the same task, and get the simulation results in the paper. Then the paper compare the difference between joint torques-time, and analyze the optimization problem of dynamic characteristics about modular industrial robots to determine which model is more suitable for 4-Dof modular industrial robots.

The input parameters

The modeling is based on the modular joints from the experiment. The dimensions of joint module are $146 \times 146 \times 293\text{mm}$, and joint weight($m_1 \sim m_4$) is 13.00kg, the effective length of link module is 54mm, and its weight is 0.8kg. Because of the symmetrical design, barycentric position of the joints are all in the geometric center. The configuration of joint module is shown in Figure 1. Z1~Z4 show the cartesian coordinate system of joints, and Generalized displacement is equal to the value of L. Thus the inertia tensor matrix I can calculated in Proe software, and the Pseudo inertia matrix can calculated by the inertia tensor matrix.

All joints are in the same plan in initial conditions. Z1~Z4 shows the cartesian coordinate system of joints, and generalized displacement is shown by L. The total height of the robot is 1094 mm. The weight of rotating joint module is 13.00kg, and the weight of link module is 0.80kg. The highest rotating speed can be reached 25rpm.

Task input parameters:

It make the input condition by the conclusion about one typical mission planning. It means that angular velocity $\dot{\theta}_i (i=1 \sim 4)$ and angular acceleration $\ddot{\theta}_i (i=1 \sim 4)$ are known. The conclusion of mission planning is shown in Figure 2. And Figure 2 shown the curves of angular displacement for each joint. Angular velocity was gained from derivative of the curves of angular displacement. The max angular displacement is 0.7rad, the max angular velocity is 1.30rad.

The angular displacement curve obtained from mission planning in Figure 2. Angular velocity was gained from derivative of the curves of angular displacement. The values of angular displacement and angular velocity curve are inputted to the Lagrange model and the Kane model in

4-Dof modular industrial robot.

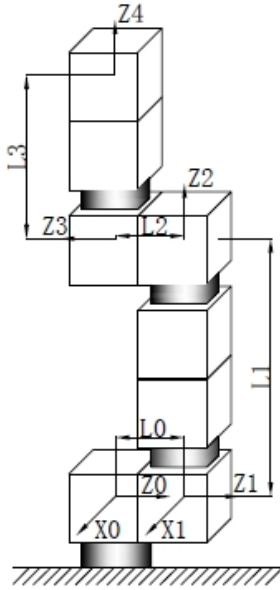


Figure 1 Configuration diagram of 4-Dof modular industrial robot

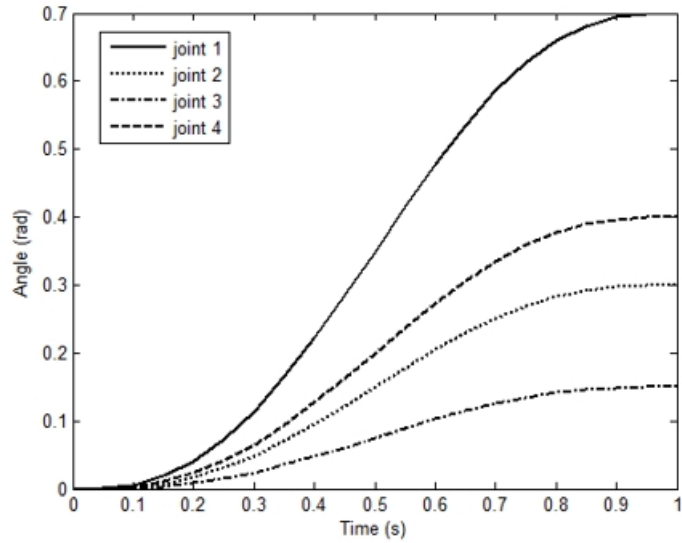


Figure 2 Inputting angular displacement curve of each joint

Establish 4-Dof dynamic model:

According to the input parameter values, Lagrange and Kane dynamic model are set up respectively. The equation of Lagrange model is T_i , in which the amount of drive inertia is ignored. $T_i = \sum_{j=1}^4 D_{ij} \ddot{q}_j + I_i(\text{act})\ddot{q}_i + \sum_{j=1}^4 \sum_{k=1}^4 D_{ijk} \dot{q}_j \dot{q}_k + D_i$. Parameters needed in modeling respectively are transformation matrix of each joint, pseudo inertia matrix, central location, quality and speed and acceleration of joints. Modeling results are as shown in Figure 3.

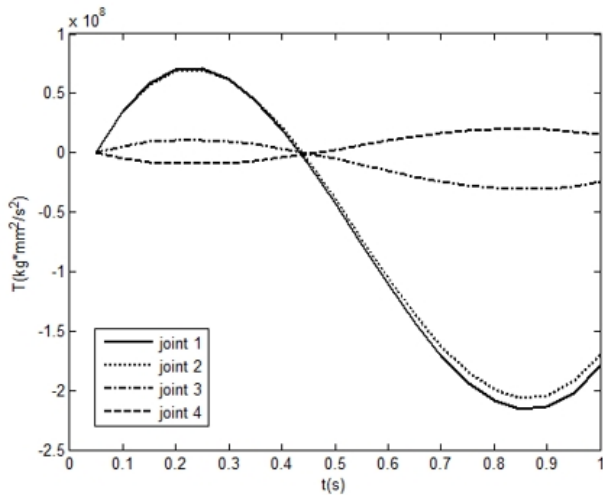


Figure 3 Torque-time simulation model results in the Lagrange

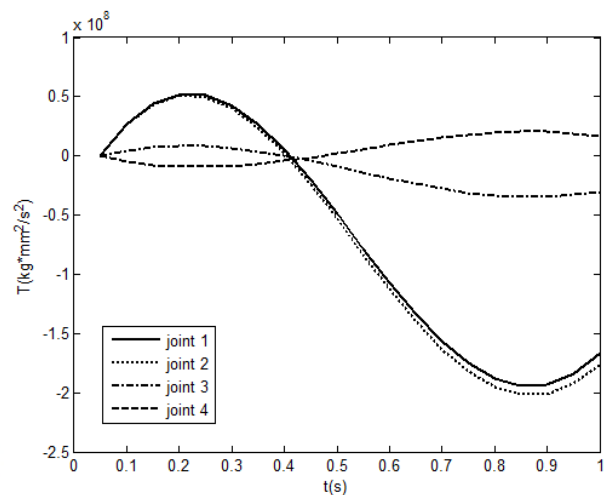


Figure 4 Torque-time simulation results in the Kane model

The equation of Kane model is $\tilde{N}_n = I_n \tilde{\omega}_n + \tilde{\omega}_n \times (I_n \cdot \tilde{\omega}_n)$, $\tau_{\theta_j} = \sum_{i=j}^n m_i \tilde{v}_{ci}^T \cdot v_{ci, \theta_j} + \sum_{i=j}^n \tilde{N}_i^T \tilde{\omega}_{i, \theta_j}$, the initial input conditions are $\omega_0 = 0, \dot{\omega}_0 = 0, v_0 = 0, \dot{v}_0 = [0 \ -g \ 0]^T, e_0 = [0 \ 0 \ 1]^T$, the parameters needed in modeling are quality, generalized displacement and inertia tensor matrix. Modeling results are shown in Figure 4.

After taking the input condition to the Lagrange model the equations are shown as follows:

$$T_1 = D_{11}\ddot{\theta}_1 + D_{12}\ddot{\theta}_2 + D_{13}\ddot{\theta}_3 + D_{111}\dot{\theta}_1^2 + D_{122}\dot{\theta}_2^2 + D_{133}\dot{\theta}_3^2 + D_{144}\dot{\theta}_4^2 + 2D_{112}\dot{\theta}_1\dot{\theta}_2 + 2D_{113}\dot{\theta}_1\dot{\theta}_3 + 2D_{114}\dot{\theta}_1\dot{\theta}_4 + 2D_{123}\dot{\theta}_2\dot{\theta}_3 + 2D_{124}\dot{\theta}_2\dot{\theta}_4 + 2D_{134}\dot{\theta}_3\dot{\theta}_4 + D_1$$

$$\begin{aligned}
T_2 &= D_{21}\ddot{\theta}_1 + D_{22}\ddot{\theta}_2 + D_{23}\ddot{\theta}_3 + D_{211}\dot{\theta}_1^2 + D_{222}\dot{\theta}_2^2 + D_{233}\dot{\theta}_3^2 + D_{244}\dot{\theta}_4^2 + 2D_{212}\dot{\theta}_1\dot{\theta}_2 \\
&\quad + 2D_{213}\dot{\theta}_1\dot{\theta}_3 + 2D_{214}\dot{\theta}_1\dot{\theta}_4 + 2D_{223}\dot{\theta}_2\dot{\theta}_3 + 2D_{224}\dot{\theta}_2\dot{\theta}_4 + 2D_{234}\dot{\theta}_3\dot{\theta}_4 + D_2 \\
T_3 &= D_{31}\ddot{\theta}_1 + D_{32}\ddot{\theta}_2 + D_{33}\ddot{\theta}_3 + D_{311}\dot{\theta}_1^2 + D_{322}\dot{\theta}_2^2 + D_{333}\dot{\theta}_3^2 + D_{344}\dot{\theta}_4^2 + 2D_{312}\dot{\theta}_1\dot{\theta}_2 \\
&\quad + 2D_{313}\dot{\theta}_1\dot{\theta}_3 + 2D_{314}\dot{\theta}_1\dot{\theta}_4 + 2D_{323}\dot{\theta}_2\dot{\theta}_3 + 2D_{324}\dot{\theta}_2\dot{\theta}_4 + 2D_{334}\dot{\theta}_3\dot{\theta}_4 + D_3 \\
T_4 &= D_{41}\ddot{\theta}_1 + D_{42}\ddot{\theta}_2 + D_{43}\ddot{\theta}_3 + D_{411}\dot{\theta}_1^2 + D_{422}\dot{\theta}_2^2 + D_{433}\dot{\theta}_3^2 + D_{444}\dot{\theta}_4^2 + 2D_{412}\dot{\theta}_1\dot{\theta}_2 \\
&\quad + 2D_{413}\dot{\theta}_1\dot{\theta}_3 + 2D_{414}\dot{\theta}_1\dot{\theta}_4 + 2D_{423}\dot{\theta}_2\dot{\theta}_3 + 2D_{424}\dot{\theta}_2\dot{\theta}_4 + 2D_{434}\dot{\theta}_3\dot{\theta}_4 + D_4
\end{aligned}$$

After taking the input condition to the Kane model the equations are shown as follows:

$$\begin{aligned}
\tau_1 &= m_1 \tilde{v}_{c1}^T \cdot v_{c1,\theta_1} + m_2 \tilde{v}_{c2}^T \cdot v_{c2,\theta_1} + m_3 \tilde{v}_{c3}^T \cdot v_{c3,\theta_1} + m_4 \tilde{v}_{c4}^T \cdot v_{c4,\theta_1} + \tilde{N}_1^T \tilde{\omega}_{1,\theta_1} \\
&\quad + \tilde{N}_2^T \tilde{\omega}_{2,\theta_1} + \tilde{N}_3^T \tilde{\omega}_{3,\theta_1} + \tilde{N}_4^T \tilde{\omega}_{4,\theta_1} \\
\tau_2 &= m_2 \tilde{v}_{c2}^T \cdot v_{c2,\theta_2} + m_3 \tilde{v}_{c3}^T \cdot v_{c3,\theta_2} + m_4 \tilde{v}_{c4}^T \cdot v_{c4,\theta_2} + \tilde{N}_2^T \tilde{\omega}_{2,\theta_2} + \tilde{N}_3^T \tilde{\omega}_{3,\theta_2} + \tilde{N}_4^T \tilde{\omega}_{4,\theta_2} \\
\tau_3 &= m_3 \tilde{v}_{c3}^T \cdot v_{c3,\theta_3} + m_4 \tilde{v}_{c4}^T \cdot v_{c4,\theta_3} + \tilde{N}_3^T \tilde{\omega}_{3,\theta_3} + \tilde{N}_4^T \tilde{\omega}_{4,\theta_3} \\
\tau_4 &= m_4 \tilde{v}_{c4}^T \cdot v_{c4,\theta_4} + \tilde{N}_4^T \tilde{\omega}_{4,\theta_4}
\end{aligned}$$

The simulation results:

With inputting the angular displacement and speed of Figure 2 to the Lagrange and Kane model, respectively, the torque - time curve of 4-Dof modular industrial robot from Lagrange method is as shown in Figure 3, and its maximum torque value appeared in 1 joints; the torque - time curve from Kane method is as shown in Figure 4, and its maximum torque value appeared in 2 joints.

Figure 5 shown the torque fluctuation of the Kane curve is smaller than the Lagrange curve, and the difference between the maximum torque values is about 45Nm. Variation range of joint angle is approximately 0.7rad. The biggest angular speed is 1.3rad/s. Figure 6 shown the torque fluctuation of the Kane curve is smaller than the Lagrange curve, and the difference between the maximum torque values is about 8Nm. Variation range of joint angle is approximately 0.4rad. The biggest angular speed is 0.75rad/s. Figure 7 shown the torque fluctuation of the Kane curve is similarity to the Lagrange curve, and the difference between the maximum torque values is about 4Nm. Variation range of joint angle is approximately 0.3rad. The biggest angular speed is 0.55rad/s. Figure 8 shown the torque fluctuation of the Kane curve is close to the Lagrange curve, and the difference between the maximum torque values is about 2Nm. Variation range of joint angle is approximately 0.15rad.

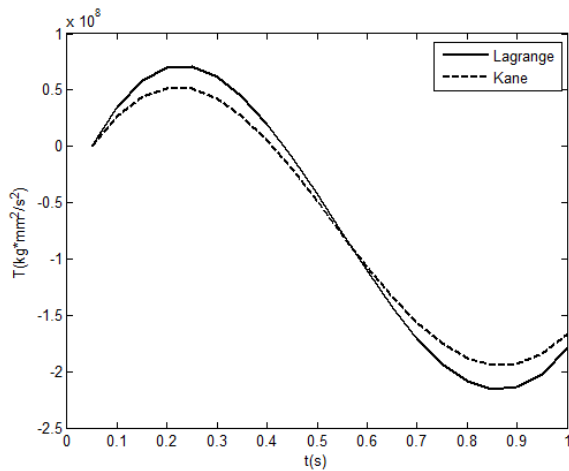


Figure 5 Torque-time curve comparison of joint 1 in the Kane model and the Lagrange model

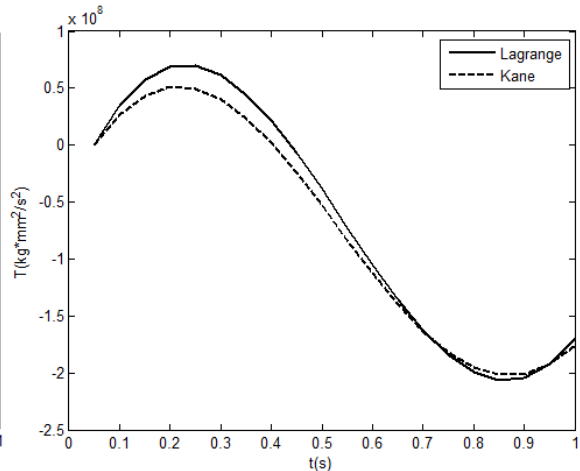


Figure 6 torque-time curve comparison of joint 2 in the Kane and the Lagrange model

The biggest angular speed is 0.25rad/s. The Curves results shown that the Kane model has better task execution effect when the joint torque is greater from Figure 5 to Figure 8.

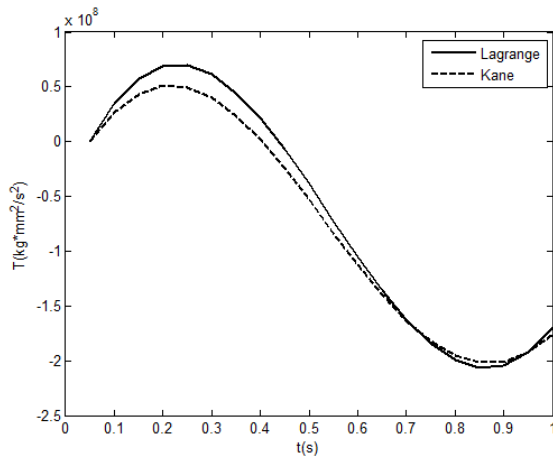


Figure 7 torque-time curve comparison of joint 2 in the Kane model and the Lagrange model

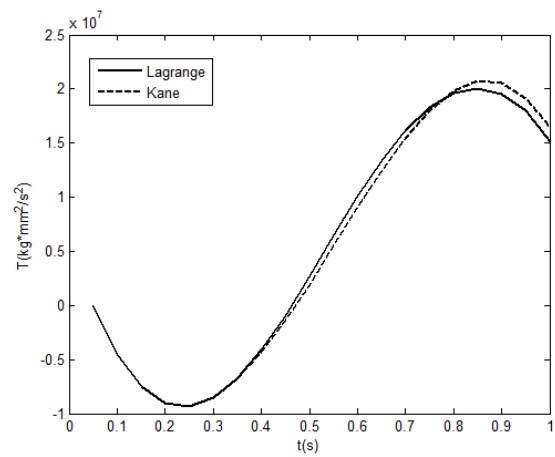


Figure 8 Torque-time curve comparison of joint 4 in the Kane model and the Lagrange model

Conclusions

The joint of new structure design has a better performance parameter. Output torque and Max speed is increased by means of different Brushless DC-Servomotor and harmonic reducer in limited interspace. The repeated positioning accuracy is not reduced when output torque and Max speed are increased. So it is an effective design method in structure deign about modular joint in modular robot.

Acknowledgements

This work was financially supported by the School of Automation, Beijing University of Posts and Telecommunication, in China.

References

- [1] De J R J, Humberto P C J, Zamudio Z, et al. Comparison of two quadrotor dynamic models[J]. Latin America Transactions IEEE, 2014, 12(4):531-537.
- [2] Zhao Y, Duan Z, Wen G. Distributed finite-time tracking of multiple Euler-Lagrange dynamics without velocity measurements[C]// Control Conference (CCC), 2013 32nd Chinese IEEE, 2013:6923-6928.
- [3] Ge X, Jin J, Ge X, et al. Dynamics Analyze of a Dual-arm Space Robot System Based on Kane's Method[C]// 2010 The 2nd International Conference on Industrial Mechatronics and Automation (ICIMA 2010) (Volume 2)2010:646-649.
- [4] Yang K, Wang X, Ge T, et al. A Dynamic model of ROV with a Robotic Manipulator Using Kane's Method[J]. IEEE, 2013:9-12.
- [5] Li Y, Xu Q. Kinematic analysis and dynamic control of a 3-PUU parallel manipulator for cardiopulmonary resuscitation[C]// Advanced Robotics, 2005. ICAR '05. Proceedings, 12th International Conference onIEEE, 2005:344-351.
- [6] Zhang X, Chen Z, Zhang X. Kinematic analysis and optimal design of a 3D compliant probe[C]// Robotics and Biomimetics (ROBIO), 2012 IEEE International Conference onIEEE, 2012:1176-1181.